# Inflight electron impact excitation in ionized metal physical vapor deposition

Junqing Lu[a)]
*Department of Mechanical and Industrial Engineering, University of Illinois, 1406 W. Green Street, Urbana, Illinois 61801*

Mark J. Kushner[b)]
*Department of Electrical and Computer Engineering, University of Illinois, 1406 W. Green Street, Urbana, Illinois 61801*

(Received 15 September 2000; accepted for publication 23 October 2000)

Ionized metal physical vapor deposition (IMPVD) is a process in which sputtered metal atoms from a magnetron target are ionized by a secondary plasma before depositing onto the substrate. The sputtered metal atoms and neutralized ions reflected from the target have higher kinetic energies than the buffer gas and so are not in thermal equilibrium. These nonthermal (inflight) species can dominate the total metal species density at low pressures ($<5$ mTorr). As a result, electron impact of the inflight species may significantly contribute to excitation and ionization. To investigate these processes, a model was developed to include the inflight electron impact excitation (IEIE) of sputtered species during IMPVD. Results for Cu IMPVD indicate that the predicted $Cu^+$ density at low pressure (2 mTorr) significantly increased when IEIE was taken into account. As the pressure increases, the rate of thermalization increases and the importance of IEIE decreases. © *2001 American Institute of Physics.* [DOI: 10.1063/1.1333026]

## I. INTRODUCTION

Ionized metal physical vapor deposition (IMPVD) is being developed to deposit metal seed layers and diffusion barriers into trenches and vias of high aspect ratio for microelectronics fabrication.[1–3] A typical IMPVD system consists of a magnetron cathode for physical sputtering of metal atoms and a secondary inductively coupled plasma (ICP) between the target and the substrate. The plasma is usually sustained in an inert gas such as Ar at moderate pressures of 10's mTorr to slow the sputtered atoms and ionize them prior to their reaching the substrate. Typical ionization fractions of the metal are 10's of percent to as large as 90%.[1] A radio frequency (rf) or dc bias may be applied to the substrate to vertically accelerate the metal ions into the wafer. The combination of anisotropic metal ions and isotropic neutral metal atoms results in conformal deposition which prevents pinch-off[1] when filling trenches.

The kinetic energy of the sputtered metal atoms from the cathode is several eV while the temperature of the background gas atoms is less than 0.1 eV. The ions which are incident onto the target have energies of 100's eV and are reflected as neutral atoms which also have kinetic energies of several eV. These high energy neutrals (sputtered atoms and reflected neutralized ions) equilibrate with the background gas through elastic collisions. Power transferred from these energetic neutrals to gas atoms during collisions produces ''sputter heating'' and ultimately rarefaction of the gas.[4] When the reactor pressure is low enough that the mean free path of sputtered and reflected neutrals is comparable to the distance between the target and the substrate, the densities of the nonthermal (inflight) species can be larger than those of thermal species. Under such conditions, electron impact excitation and ionization of the inflight species become important. This mechanism may be particularly important in ionized hollow cathode magnetron sputtering devices, which typically operate below 10 mTorr.[5]

In this paper, we present results from an investigation of the electron impact excitation of inflight species during Cu IMPVD. The computational platforms used in this study are the two-dimensional Hybrid Plasma Equipment Model (HPEM) (Refs. 6,7) and the Monte Carlo Feature Profile Model (MCFPM).[8] The HPEM has been previously validated for the IMPVD conditions of interest.[7] The effect of inflight electron impact excitation (IEIE) was numerically investigated as a function of pressure from 2 to 40 mTorr by incorporating IEIE algorithms into the HPEM. We note that IEIE is an integrated part of the plasma physics in an experiment and cannot be ''toggled'' on and off. In numerical studies such as this, however, the model can be run with and without the IEIE algorithms to determine the physical significance of IEIE. It was found that at low pressure ($\approx$2 mTorr) IEIE can increase the predicted $Cu^+$ density by as much as a factor of 2, and that the effect of IEIE diminishes with increasing pressure as the rate of thermalization of the inflight species increases. The consequence of IEIE can be seen in the profiles of microtrenches filled using IMPVD.

## II. DESCRIPTION OF THE MODEL

The HPEM has been previously described in detail.[6,7] The HPEM is a modular simulator which iteratively achieves a quasisteady state solution. The modules used here are the

[a)]Electronic mail: j-lu@uiuc.edu
[b)]Electronic mail: mjk@uiuc.edu

 

electromagnetic module (EMM), the electron energy transport module (EETM), and the fluid kinetics simulation (FKS). Inductively coupled electromagnetic fields and magnetostatic fields are computed in EMM. These fields are then used in EETM to solve the electron energy equation for the temperature of bulk electrons. Using Monte Carlo techniques, the trajectories of secondary electrons emitted from the cathode are followed and their electron energy distributions are obtained. The electron temperatures and energy distributions are used to generate sources for electron impact processes and electron transport coefficients. These rates and coefficients are then used in the FKS where continuity, momentum, and energy equations are integrated for all heavy particles (neutrals and ions). Poisson's equation is solved for the plasma potential throughout the reactor. The sputter transport algorithms are included in the FKS. Densities and electric fields are then transferred to the EMM and EETM, and the process is repeated until a converged solution is obtained. The gas pressure was held constant at the specified value by throttling the pump rate. The electron transport in radial and axial directions is resolved within each rf period. The electron motion in the azimuthal direction is not resolved in the fluid modules, but is tracked in the Monte Carlo modules. The species densities shown here are averaged over several rf periods.

The transport of the sputtered and reflected atoms is modeled by Monte Carlo techniques and is described in detail in a previous publication.[7] Only the electron impact excitation of nonthermal species will be described in detail here. Using a cascade distribution for the energy of sputtered atoms, pseudoparticles are emitted from the target and their trajectories are integrated using Monte Carlo methods. The mean free path of the energetic neutrals is determined using null collision techniques to account for spatially dependent gas properties (density and composition) resulting from, for example, gas heating and changes in composition due to slowing down of energetic neutrals. A probability array is constructed for collisions between the energetic neutral and other species, including electrons. A random number is generated to determine the collision partner. When the collision partner is an electron, a second probability array is constructed based on the local electron temperature to determine the electron impact reaction that occurs and the product. The effective probability $p_i$ for $i$th reaction is based on the rate coefficient $k_i$ for electron impact,

$$p_i = \frac{k_i(T_e)}{v_{\text{th}}}, \tag{1}$$

where $v_{\text{th}}$ is the random thermal speed of the electron. These probabilities are added and normalized to 1. A random number is generated to determine which reaction occurs. Since the momentum transferred to the gas atom during an electron impact is small, the pseudoparticle retains its original velocity following electron elastic and excitation collisions, and the particle is tracked until it thermalizes or strikes a surface. The rates of thermalization of neutral species are recorded into source terms for incorporation into the fluid continuity equations. For electron impact collisions producing ions, the pseudoparticles are removed from the sputter calculation. Ion source terms are generated at the location of ionization and incorporated into the fluid continuity equations. Due to the strong electrostatic forces in the plasma, the ions rapidly equilibrate with the bulk ions. The trajectories of the inflight metal atoms are recorded to obtain the inflight species densities.

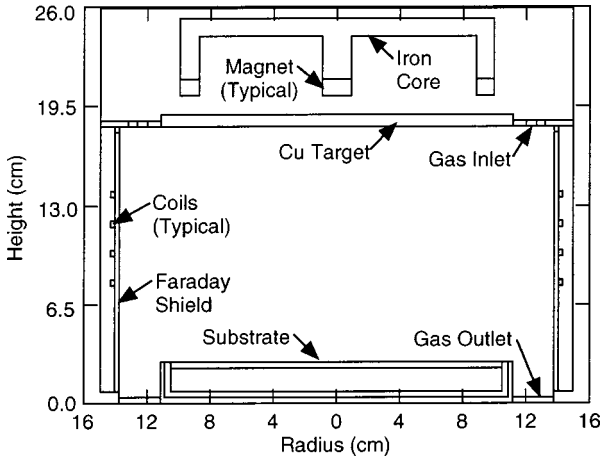


FIG. 1. Schematic of an IMPVD reactor with external coils and a Faraday shield.

To assess the consequences of IEIE on profile evolution of trenches filled with metal using IMPVD, the MCFPM was used. The MCFPM was first developed to simulate etch profiles using the flux distributions produced by HPEM.[8] The MCFPM resolves the trench region on the wafer using a rectilinear mesh, with typical mesh spacing of 100 cells for 1.0 $\mu$m length. One solid cell represents the width of several hundred atoms. Each cell is assigned a material identity, which may change during the simulation. Gas phase species are represented by pseudoparticles. The solid materials are represented by computational cells. Pseudoparticles are launched from random locations above the trench, with energy and angles sampled from the flux distributions produced by the HPEM. The trajectories of these particles are tracked until they hit the solid material. Depending on the gas–solid reaction mechanism, either etching or deposition occurs, and the identity of the computational cell is changed accordingly.

## III. INFLIGHT ELECTRON IMPACT EXCITATION

The IMPVD reactor used in this investigation is shown in Fig. 1. The reactor has a conventional magnetron at the top and a substrate 15 cm below the Cu target. The diameters of the target and substrate are 22 and 21 cm, respectively. The rf inductive power is supplied by a four-turn coil outside of the plasma through a Faraday shield.[9] Computationally, the azimuthal electric field is allowed to simply propagate through the Faraday shield. The operating conditions are 0.5 kW ICP power, 1.0 kW magnetron power, and 2–40 mTorr Ar. For example, at 20 mTorr, the peak electron density is $5.3\times10^{11}$ cm$^{-3}$, target voltage is 253 V, and electron temperature is 3.2–3.8 eV. HPEM predictions with and without IEIE were compared to quantify the effect of inflight processes.

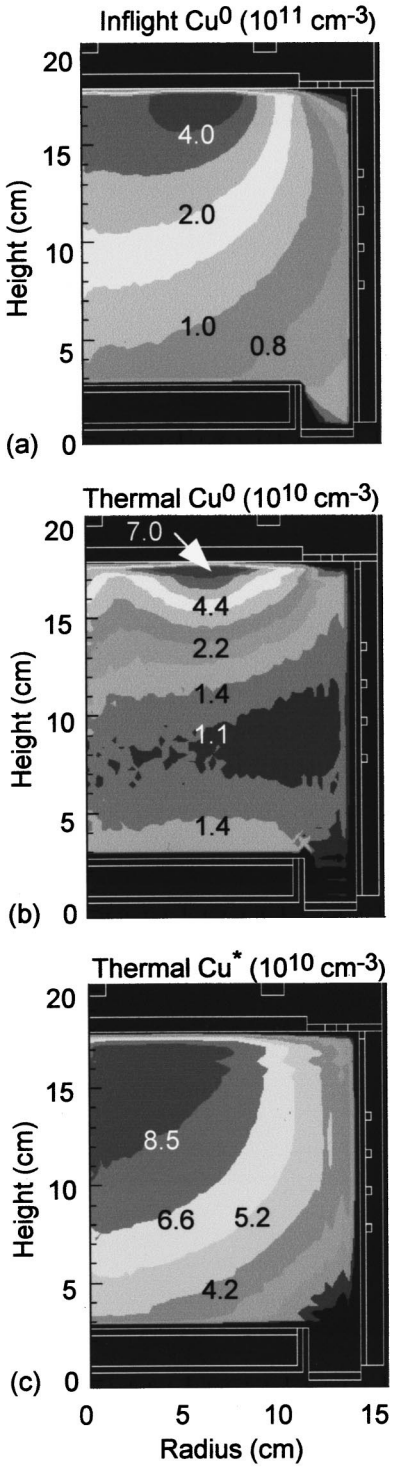


FIG. 2. Predicted Cu species with IEIE at 2 mTorr. (a) Inflight $Cu^0$ density, (b) thermal $Cu^0$ density, and (c) thermal Cu* density. The majority of the Cu species are inflight.

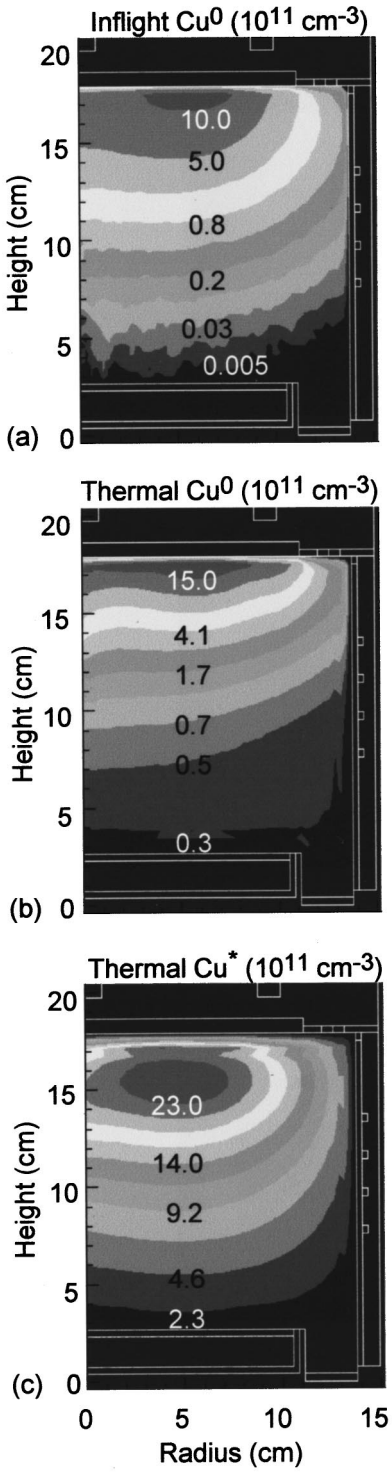


FIG. 3. Predicted Cu species with IEIE at 40 mTorr. (a) Inflight $Cu^0$ density, (b) thermal $Cu^0$ density, and (c) thermal Cu* density. The majority of the Cu species are thermalized.

The temperature of the Ar buffer gas at 2 mTorr is about 1000 K due to heating from the ICP and the magnetron power. Under these conditions, the mean free path for Cu–Ar elastic collisions is 20 cm which is commensurate with the reactor dimensions. The majority of the sputtered Cu atoms therefore undergo few collisions before reaching the substrate. As a consequence, the dominant Cu species at 2 mTorr should be the inflight Cu atoms. For example, the predicted Cu species densities with IEIE at 2 mTorr are shown in Fig. 2. The inflight Cu ground state density (denoted by $Cu^0$) peaks at $4.0\times10^{11}$ $cm^{-3}$ below the target, and decreases to $8\times10^{10}$ $cm^{-3}$ above the wafer. This decrease is in part due to thermalizing collisions and in part due to the diverging trajectories of the sputtered Cu atoms originating from the narrow sputter track beneath the cusp of the mag-

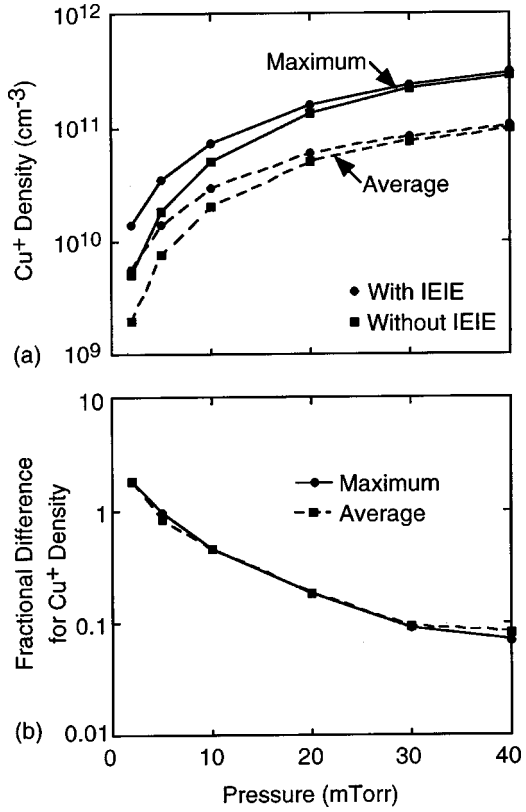


FIG. 4. Predicted $Cu^+$ densities as a function of pressure with and without IEIE. (a) Maximum and reactor-averaged values and (b) fractional differences. The differences are large at low pressures (<20 mTorr).

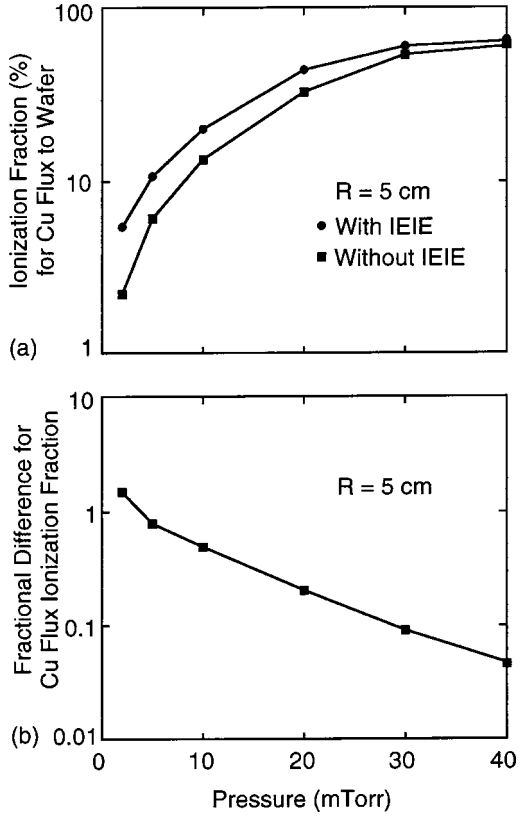


FIG. 5. Predicted ionization fractions of the Cu flux to wafer at a radius of 5 cm with and without IEIE. (a) Ionization fractions and (b) fractional difference. The differences are large at low pressures (<20 mTorr).

net. The thermal $Cu^0$ density is about an order of magnitude less than the inflight $Cu^0$ density, ranging from 1.1 to 7.0 $\times 10^{10}$ $cm^{-3}$. The thermal Cu* [nominally the Cu($^2D$) state] ranges from 2.2 to $8.5\times 10^{10}$ $cm^{-3}$ between the target and the substrate and is large near the cusp of the magnet where total excitation rates peak. The inflight $Cu^0$ density is about 2 times the sum of the thermal $Cu^0$ and Cu* densities. The inflight Cu* density (not shown) ranges from $1.0\times 10^9$ $cm^{-3}$ to $2.0\times 10^8$ $cm^{-3}$, 2–3 orders of magnitude smaller than the inflight $Cu^0$ density. Besides contributions for direct ionization of inflight Cu atoms, multistep ionization is also important. The average Cu* density with IEIE is $4.6\times 10^{10}$ $cm^{-3}$, 3 times that without IEIE. Since Cu* is metastable and has a lower ionization potential than Cu, approximately 15% of total ionization comes from electron impact of Cu*.

As the pressure increases, the density of inflight species decreases due to the shorter mean free path and more rapid thermalization. At high enough pressures (>20 mTorr), the Cu species are largely thermalized. For example, the predicted Cu species densities at 40 mTorr are shown in Fig. 3. The inflight $Cu^0$ density ranges from $1.0\times 10^{12}$ $cm^{-3}$ below the target to $5.0\times 10^8$ $cm^{-3}$ above the wafer, indicating almost total thermalization. The inflight Cu* densities, not shown here, are on the order of $10^8$ $cm^{-3}$, much lower than the inflight $Cu^0$ density. The thermal $Cu^0$ density ranges from $1.5\times 10^{12}$ $cm^{-3}$ below the target to $3.0\times 10^{10}$ $cm^{-3}$ above the wafer, becoming increasingly larger than the inflight $Cu^0$ density from the target to wafer. The ratio of thermal to inflight $Cu^0$ increases from target to substrate, reflecting the transition from inflight to thermal as the inflight $Cu^0$ atoms undergo collisions. The Cu* density, ranging from 2.3 $\times 10^{12}$ $cm^{-3}$ to $2.3\times 10^{11}$ $cm^{-3}$ (above the wafer), exceeds the $Cu^0$ due to the low rate of quenching and low mobility of Cu* at the higher pressure.

The predicted $Cu^+$ density is significantly affected by IEIE. For example, the maximum and the reactor averaged $Cu^+$ densities are shown in Fig. 4(a), with and without IEIE. The $Cu^+$ densities with IEIE are larger than those without IEIE, for both the maximum and the reactor averaged densities. The difference is largest at the lowest pressure of 2 mTorr, and decreases as pressure increases. Note that for these cases the magnetron and ICP power are held constant, thereby ''fixing'' the ion density. Although the $Cu^+$ density may vary, the total ion density does not as the more numerous $Ar^+$ ions ($[Ar^+]/[Cu^+]\approx 3.0$ at 20 mTorr) change their density to compensate. The fractional difference for the $Cu^+$ density with and without IEIE is shown in Fig. 4(b). The fractional difference is defined as $([Cu^+]-[Cu^+]_0)/[Cu^+]_0$, where $[Cu^+]$ is the density with IEIE, and $[Cu^+]_0$ is the density without IEIE. At the same pressure, the fractional differences are essentially the same for the maximum and the average values. The fractional difference, 1.8 at 2 mTorr, monotonically decreases with pressure and is 0.1 at 40 mTorr. This indicates that IEIE is the dominant source of ionization for Cu at low pressure and is not negligible (10%) even at the relatively high pressure of 40 mTorr.

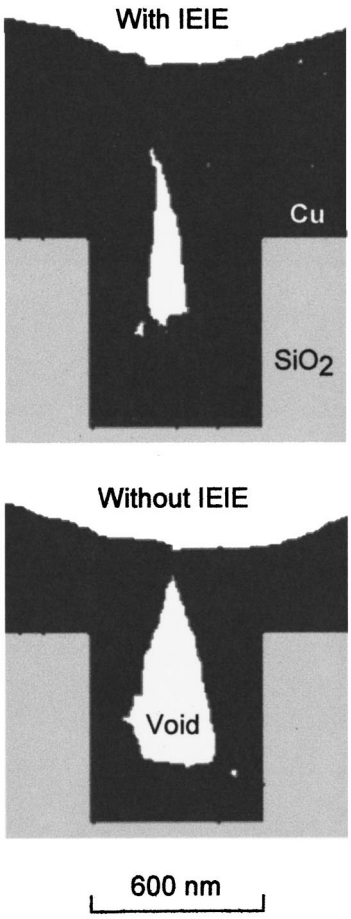


FIG. 6. Predicted trench profiles for Cu deposition with and without IEIE at 20 mTorr. The increased Cu ionization fraction with IEIE reduces the size of the void due to an increase in the ionization fraction of the incident metal ion flux.

The predicted ionization fraction of the Cu flux to wafer [ion flux/total flux] is also significantly modified by IEIE at low pressure (<20 mTorr) as shown in Fig. 5. Fluxes are shown for a radius of 5 cm on the wafer which is representative of the total metal flux to wafer. The ionization fractions increase with pressure (from 6% at 2 mTorr to 66% at 40 mTorr, with IEIE), consistent with the $Cu^+$ densities in Fig. 4(a). The Cu flux ionization fraction at 2 mTorr is 150% larger with IEIE than that without. As the pressure increases, the fractional difference [(with IEIE−without IEIE)/without IEIE] in the flux ionization fraction decreases to only 5% at 40 mTorr. The effect of IEIE on the ionization fraction of the depositing metal flux is similar to that on $Cu^+$ densities.

Although it is difficult to experimentally isolate the consequences of IEIE, one can numerically demonstrate those effects on deposition profiles. For example, profiles for Cu trench filling obtained with the MCFPM at 20 mTorr using fluxes from the HPEM with and without IEIE are shown in Fig. 6. In IMPVD, the ionization fraction of the depositing flux typically increases with increasing pressure in the few to tens of mTorr range. Larger ionization fractions tend to produce more conformal depositions due to both more direct filling (metal ions in the depositing flux have a narrower angular distribution than neutrals) and sputtering of deposits at the top edges of the trench which would otherwise overlap to produce ''keyhole'' voids. At 20 mTorr the ionization fraction is sufficiently low that, for these process conditions, a void is produce. When including IEIE, a smaller void is produced because the Cu flux with IEIE has a larger ionization fraction (43%) than that without IEIE (33%). Under similar conditions, experimental observations[10] suggest that the large void without IEIE is likely to occur at a lower pressure of 5 mTorr since the ionization fraction is lower. The small void at 20 mTorr predicted with IEIE is more consistent with experimental observations.

The majority (>90%) of the incident ion flux to the target is $Ar^+$. These $Ar^+$ reflect from the target as fast Ar neutrals with an average energy of 6 eV.[11] Hence, there is a significant amount of inflight Ar species in the plasma in addition to the inflight Cu species. However, the $Ar^+$ densities with and without IEIE are essentially the same at all pressures. The fixed target power of 1 kW is the major controlling factor for $Ar^+$, which makes up the majority of the ion flux. The constant magnetron power maintains an essentially constant $Ar^+$ density independent of IEIE.

## IV. CONCLUDING REMARKS

In conclusion, inflight electron impact excitation (IEIE) contributes significantly to the density of metal ion species and the ionization fraction of the depositing metal flux at low and moderate pressures. At the high plasma densities of IMPVD systems, even inflight atoms which have short thermalization distance (or transit times) can be ionized or excited. The density of the buffer gas ions is controlled by the magnetron power, and is relatively independent of IEIE.

## ACKNOWLEDGMENTS

This work was supported by the Semiconductor Research Corporation, National Science Foundation (CTS99-74962) and DARPA/AFOSR and Applied Materials Corp.

[1] S. M. Rossnagel, Semicond. Int. **21**, 99 (1996).
[2] S. M. Rossnagel and J. Hopwood, J. Vac. Sci. Technol. B **12**, 449 (1994).
[3] C. Ryu, H. Lee, K. W. Kwon, A. L. S. Loke, and S. S. Wong, Solid State Technol. **42**, 53 (1999).
[4] S. M. Rossnagel, J. Vac. Sci. Technol. B **16**, 3008 (1998).
[5] E. Klawuhn, G. C. D'Couto, K. A. Ashtiani, P. Rymer, M. A. Biberger, and K. B. Levy, J. Vac. Sci. Technol. A **18**, 1546 (2000).
[6] M. J. Grapperhaus, Z. Krivokapic, and M. J. Kushner, J. Appl. Phys. **83**, 35 (1998).
[7] J. Lu and M. J. Kushner, J. Appl. Phys. **87**, 7198 (2000).
[8] R. J. Hoekstra, M. J. Grapperhaus, and M. J. Kushner, J. Vac. Sci. Technol. A **15**, 1913 (1999).
[9] R. Bayer, A. D. Lantsman, and J. A. Seirmarco, U. S. Patent No. 5 569 363 (filed 1996).
[10] P. F. Cheng and S. M. Rossnagel, J. Vac. Sci. Technol. B **13**, 203 (1995).
[11] J. D. Kress, D. E. Hanson, F. F. Voter, C. L. Liu, X. Y. Liu, and D. G. Coronell, J. Vac. Sci. Technol. A **17**, 2819 (1999).